

# Optimum vegetation height and density for inorganic sedimentation in deltaic marshes

William Nardin<sup>1,2\*</sup> and Douglas A. Edmonds<sup>1\*</sup>

**River deltas support a disproportionate percentage of the world's population and some are drowning as sea level rises<sup>1</sup>. Resilient deltas theoretically balance relative sea-level rise with vertical growth from surface sedimentation<sup>2-7</sup>. Vegetation generally enhances inorganic sedimentation and resiliency in some settings, such as tidal saltwater marshes<sup>8</sup>, but the effect of vegetation on freshwater marshes in river deltas is less clear. Here we use a hydrodynamic numerical model<sup>9</sup> to simulate deposition in a river delta with varying vegetation characteristics and water discharge and show that vegetation does not always enhance sedimentation on a freshwater marsh. For a given flood, we find that intermediate vegetation height and density are optimal for enhancing both sand and mud deposition, whereas tall or dense vegetation causes sand to remain in the river channel, reducing marsh sedimentation. A multivariate regression analysis of remote-sensing data from Wax Lake Delta, Louisiana, USA shows that the delta exhibits a hydrodynamic response to vegetation in agreement with model predictions. Because most sediment is delivered to freshwater deltaic marshes by infrequent storm and flood events, we further suggest that the timing of such events relative to seasonal vegetation growth determines the integrated effect of vegetation on delta resiliency.**

The presence of vegetation on inundated surfaces can enhance inorganic sedimentation because vegetation physically traps sediment<sup>10</sup>; slows flow, leading to sediment deposition<sup>11</sup>; and enhances substrate stability, preventing erosion<sup>12</sup>. These processes are particularly important in creating resilient coastal marshes. For example, tidally dominated coastal salt marshes are resilient landforms because as tidal inundation increases owing to sea-level rise, vegetation growth (and therefore sedimentation) increases<sup>8,11</sup>—although only to a point<sup>13</sup>. It is not clear how these ecogeomorphic feedbacks apply to deltaic freshwater marshes whose vertical accretion is inextricably linked to fluvial inundation<sup>14,15</sup> in addition to tidal and storm processes. At present there is scant evidence that vegetation enhances sedimentation in freshwater deltaic marshes<sup>12,15</sup>. For sedimentological restoration strategies in deltas<sup>16</sup> to be successful we need to understand the interaction between vegetation and sedimentation.

Our goal is to understand how vegetation influences inorganic sedimentation in freshwater deltaic marshes dominated by flooding by using numerical experiments with Delft3D (v. 4.00.01) and remote-sensing data. For this study we focus only on inorganic sedimentation because it constructs the platform on which vegetation grows and is usually the dominant sediment type in deltaic systems. Our simulations are non-morphodynamic because we are focusing only on deposition during a flood. Typical

deposition in model runs is  $\sim 10$  cm, and would have a minimal effect on morphodynamics. We model floods using a peak flood discharge, rather than the time-dependent wave, because most sediment transport occurs around peak flow.

We conducted 75 simulations varying vegetation height and density, and water discharge. Each simulation starts from the same pre-formed river delta (Fig. 1 and see Methods for model set-up). The pre-formed delta was created with a steady discharge of  $1,250 \text{ m}^3 \text{ s}^{-1}$ , carrying equilibrium concentrations of  $100 \mu\text{m}$  non-cohesive sediment (defined as diameter  $> 64 \mu\text{m}$ ) and  $25 \mu\text{m}$  aggregated cohesive sediment (defined as diameter  $< 64 \mu\text{m}$ ). On the pre-formed delta, we define surfaces above sea level as marsh (for example, Fig. 1) and populate those surfaces with vegetation of a given height  $h_v$ , density  $n$ , and drag coefficient on the stems  $C_D$  (assumed constant at 1.65). In our runs  $h_v$  varies from 0.05 to 1.5 m and  $n$  from 0.05 to  $0.5 \text{ m}^{-1}$ . We subject each combination of  $h_v$  and  $n$  to flood discharges ( $Q_f$ ) of 2,500, 3,750 and  $5,000 \text{ m}^3 \text{ s}^{-1}$  (Supplementary Table 1). To compare runs, we define non-dimensional vegetation height as  $\hat{h}_v = h_v / \bar{D}$  where  $\bar{D}$  is the spatially averaged water depth on deltaic marsh surfaces for a given run. A control run with no vegetation is computed for each  $Q_f$ .

To account for the effects of vegetation on flow and sediment transport we implement the analytical equations proposed in ref. 17 in Delft3D because these equations can be used in depth-integrated models—as opposed to more complicated equations for three-dimensional models<sup>18</sup>—and they also agree well with experimental and field data<sup>19-21</sup> (see Supplementary Information for model validation discussion). This method treats vegetation stems as uniformly spaced rigid vertical cylinders. Flow velocity through the stems is assumed to be uniform. The model does not include particle capture by vegetation stems because, at least in tidal marshes<sup>22</sup>, it is a secondary mechanism.

The effect of vegetation is parameterized through the flow resistance, with separate expressions for flow resistance due to submerged ( $\hat{h}_v < 1$ ) and non-submerged ( $\hat{h}_v > 1$ ) vegetation. Vegetation on an inundated bed causes flow resistance, which steepens the water surface slope and increases the depth. The basal shear stress in the presence of vegetation is partitioned into that which acts on the bed and on the vegetation. The shear stress acting on the vegetation results in momentum loss, which reduces the basal shear stress on a vegetated bed (see Supplementary Information for derivation).

We first focus on how  $\hat{h}_v$ ,  $n$  and  $Q_f$  affect the water flux through all marsh surfaces on the delta. The marsh water flux is a property of first-order interest because it partly controls biogeochemical filtering (for example, denitrification)<sup>23</sup>, and sedimentation potential. We quantify the water flux ( $Q$ ,  $\text{m}^3 \text{ s}^{-1}$ ) ratio for vegetated (v) or non-vegetated (nv) conditions as  $R_w = Q_v / Q_{nv}$ .

<sup>1</sup>Indiana University, Department of Geological Sciences and Center for Geospatial Data Analysis, Bloomington, Indiana 47405, USA, <sup>2</sup>Boston University, Department of Earth and Environment, Boston, Massachusetts 02215, USA. \*e-mail: [wnardin@bu.edu](mailto:wnardin@bu.edu); [edmondssd@indiana.edu](mailto:edmondssd@indiana.edu)

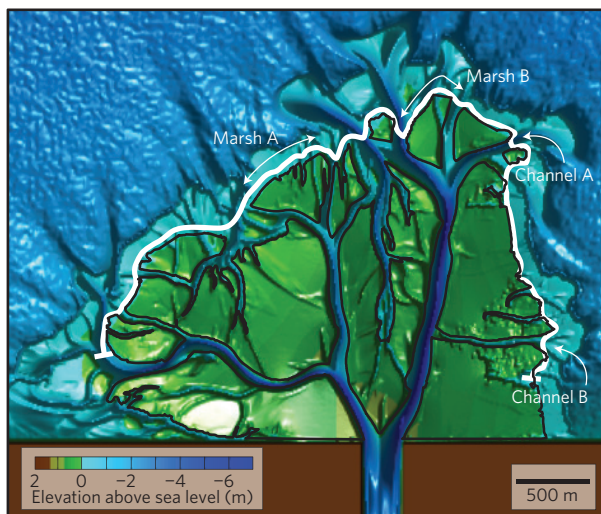


**Figure 1 | Plan view image of the delta configuration used in this study.**

The shaded relief map of bathymetry shows the delta morphology generated by Delft3D. Solid black lines enclose individual marsh platforms (at an elevation of 0 m) where water and sediment mass balance calculations were made. The solid white line shows the portion of shoreline in Fig. 2c. See Methods for how shoreline is defined.

In our results we find that for a given  $Q_f$ , increasing  $\hat{h}_v$  and  $n$  increases water in the channels and reduces  $R_w$  on marsh surfaces by up to 40% (Fig. 2a). This arises because vegetation increases marsh surface roughness, and water seeks less resistant paths through the channels, similar to observations in flume experiments<sup>24</sup> and tidal channels<sup>25</sup>. For a given  $\hat{h}_v$  and  $n$ , increasing  $Q_f$  has minimal effect on  $R_w$ .

To see why vegetation decreases marsh water flux, consider that  $R_w$  is set by the average water depth and velocity on all marsh surfaces; marsh width does not play a role because it is not changing.

Calculating analogous ratios for spatially averaged depth ( $\bar{D}$ ) and velocity ( $\bar{U}$ ) where  $R_D = \bar{D}_v/\bar{D}_{nv}$  and  $R_U = \bar{U}_v/\bar{U}_{nv}$ , we find that on marsh surfaces roughness from vegetation increases  $R_D$ , and reduces  $R_U$  (Fig. 2b). As  $R_U$  reduces more than  $R_D$  increases there is an overall reduction in  $R_w$  and therefore an increase in channel water flux. For example,  $R_w > 1$  at the channel mouths and  $R_w < 1$  at the marsh shorelines, indicating that larger  $\hat{h}_v$  increases the water (and sediment) flux through the channels that bypasses the marsh surfaces and exits to sea (Fig. 2c).

To quantify differences in marsh sedimentation we calculate the sedimentation ratio ( $R_s$ ) for vegetated relative to non-vegetated conditions for non-cohesive sand (nc) and cohesive mud (coh) on all marsh platforms, where  $R_{S(nc \text{ or } coh)} = (Q_{si} - Q_{so})_v / (Q_{si} - Q_{so})_{nv}$ .  $Q_{si}$  and  $Q_{so}$  are the sums of incoming and outgoing sediment fluxes ( $\text{kg s}^{-1}$ ) for all marsh surfaces, respectively.

Interestingly, for all parameters tested an intermediate  $\hat{h}_v$  maximizes non-cohesive sedimentation within the marsh (Fig. 3a). We also tested other delta configurations and found similar peaks (Supplementary Information). As  $n$  decreases and  $Q_f$  increases, the peak in  $R_{S(nc)}$  shifts to progressively higher  $\hat{h}_v$  and increases in magnitude.  $R_{S(nc)}$  reaches a maximum of  $\sim 1.5$  for  $\hat{h}_v$  of  $\sim 0.25$  and  $n$  of 0.05. At  $\hat{h}_v > \sim 1$ ,  $R_{S(nc)}$  is less than one for all conditions tested, indicating that the presence of vegetation reduces non-cohesive sedimentation. Remarkably, in our model runs this effect decreases sedimentation by 30–80% compared with non-vegetated marsh platforms (Fig. 3a).

To understand this depositional signature, we define the incoming concentration ratio ( $R_c$ ) such that  $R_{c(nc \text{ or } coh)} = (Q_{si}/Q_v) / (Q_{si}/Q)_{nv}$ . The maximum in  $R_{S(nc)}$  occurs because an intermediate value of  $\hat{h}_v$  maximizes the  $R_{c(nc)}$  of water delivered to the marsh (Fig. 3b). This occurs at intermediate  $\hat{h}_v$  because the presence of vegetation forces more water into the bordering channels (Fig. 2a), which increases the channelized velocity (Fig. 2c) and sedimentation concentration (Fig. 3b), yet, the marsh-directed velocity is still large enough to transport non-cohesive sediment into marsh.  $R_{c(nc)}$  is less at low and high  $\hat{h}_v$ , because at low  $\hat{h}_v$  the marsh water flux is high but the channel velocity is relatively low,

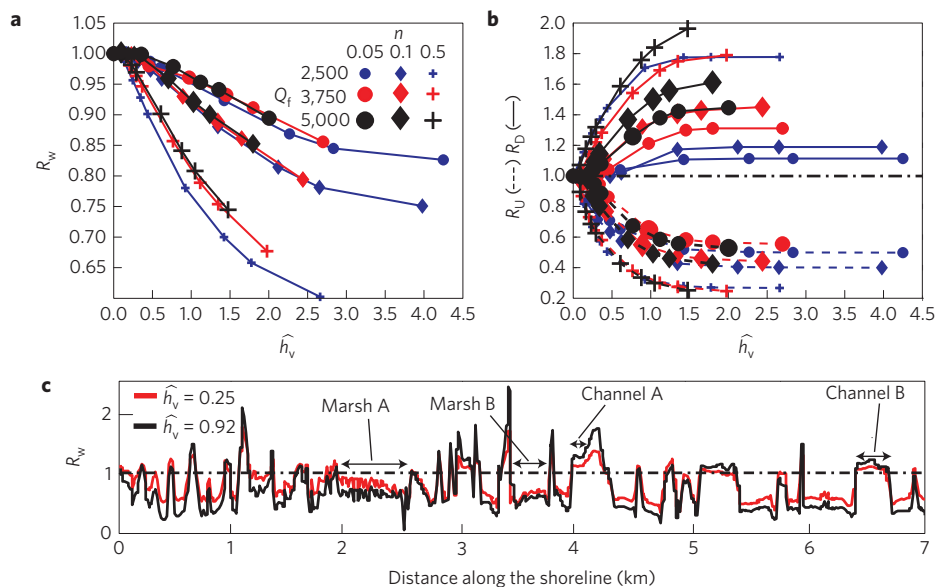


**Figure 2 | Modelled water fluxes under vegetated and non-vegetated conditions.** **a**, Water fluxes in the presence of vegetation relative to no vegetation ( $R_w$ ) decrease with increasing non-dimensional vegetation height ( $\hat{h}_v$ ). The inset plot defines flood discharge ( $Q_f$ ) and vegetation density ( $n$ ) for each symbol. **b**, Normalized average water depths ( $R_D$ ) and velocities ( $R_U$ ) increase and decrease, respectively, with increasing  $\hat{h}_v$ . There is minimal change when  $\hat{h}_v > 1$  because the vegetation is no longer submerged. **c**, Vegetation increases  $R_w$  in channels whereas it decreases  $R_w$  over the marsh surfaces when measured at the shoreline. Shoreline location is shown in Fig. 1.

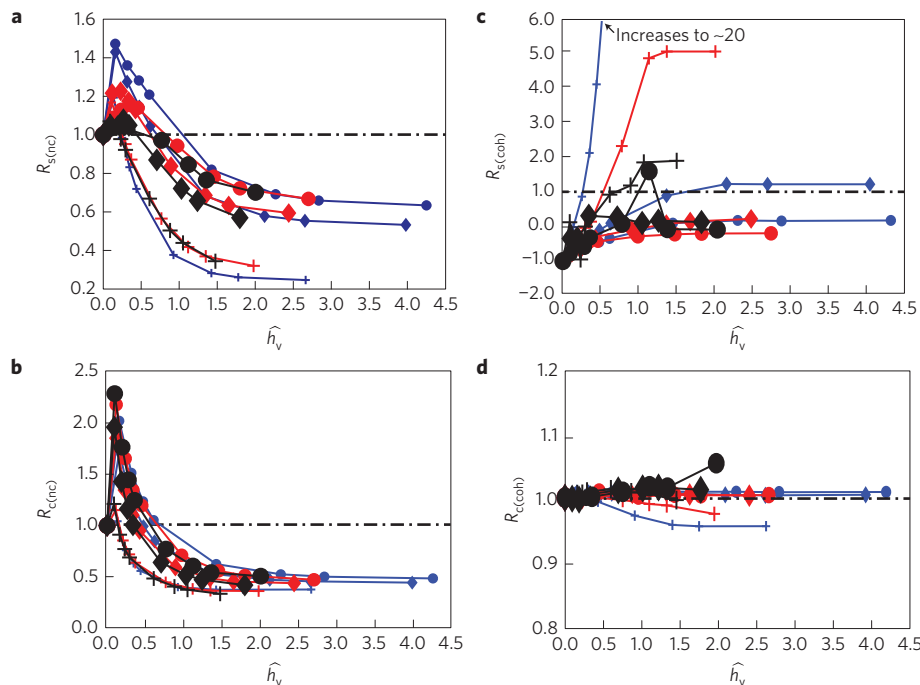


**Figure 3 | Modelled sediment fluxes for marsh platforms under vegetated and non-vegetated conditions. a, b,** Both non-cohesive sedimentation and concentration ratios,  $R_{S(nc)}$  and  $R_{c(nc)}$  respectively, increase as a function of  $\hat{h}_v$  and then decrease. **c,** Cohesive sedimentation ratio,  $R_{S(coh)}$ , generally increases as a function of  $\hat{h}_v$ , although it becomes greater than 1 when the depositional threshold is met. Negative values represent erosion. **d,**  $R_{c(coh)}$  is generally constant for all runs. See the inset plot in Fig. 2a for mapping between run symbols, and  $Q_f$  and  $n$ .

and at high  $\hat{h}_v$ , the channel velocity is high but the marsh water flux is low.

Cohesive sediment behaves differently. At  $\hat{h}_v < \sim 0.2$  there is net erosion of cohesive sediment from deltaic marshes for all conditions tested due to high flow velocity over the marsh surfaces (Fig. 3c). However, at larger values of  $\hat{h}_v$  there is divergent behaviour where some runs have reduced sedimentation where  $0 < R_{S(coh)} < 1$ , and some have enhanced sedimentation where  $R_{S(coh)} > 1$ . In this case, the relative concentrations of cohesive sediment entering the marsh ( $R_{c(coh)}$ ) stay the same (Fig. 3d), and the divergence arises because cohesive sediment deposition<sup>26</sup> occurs when bed shear stress is reduced below a threshold (in our runs we set this to 0.25 Pa). For large values of  $n$  and low values of  $Q_f$ , velocity and shear stress are reduced below the critical value and  $R_{S(coh)}$  increases strongly with increasing  $\hat{h}_v$  because the vegetation increases water residence time, trapping more cohesive sediment. Conversely, increasing  $Q_f$  and decreasing  $n$  keeps  $R_U$  relatively high on the marsh and this minimizes  $R_{S(coh)}$ . These results suggest that for cohesive sediment, if the depositional threshold has been met, then the presence of vegetation should enhance deposition.

To test our results we used linear multivariate regression to determine whether vegetation increases water level in Wax Lake Delta, Louisiana, USA, a result we observed in our model runs ( $R_D$  in Fig. 2b). We gathered water level elevation ( $WL$ , m) at the head of Wax Lake Delta, incoming discharge ( $Q_{in}$ ,  $m^3 s^{-1}$ ), tidal elevation ( $T$ , m), and vegetation data ( $V$ , unitless). We used the normalized difference vegetation index (NDVI) as a proxy for  $V$  (see Methods for more details). Our analysis indicates that  $WL = 0.11V + 0.32T + 0.000075Q_{in} + 0.21$  (all coefficients are significant with  $p < 0.05$ , Supplementary Table 2). In our data set, vegetation accounts for  $\sim 3$ –5% of  $WL$  variance, and its presence increases  $WL \sim 10\%$  on average, similar to runs with low  $\hat{h}_v$  and/or low  $Q_f$  and  $n$  (Fig. 2b).

Previous work on tidal salt marshes has shown that vegetation generally enhances sedimentation and resiliency<sup>8</sup>, but our results

suggest that may not be true for deltaic marshes. First consider that vegetation affects sand and mud deposition differently and, in contrast to most tidal systems, both sand and mud are critical for maintaining deltas. After all, deltas such as the Mississippi and Wax Lake are composed of 50–70% sand even though the incoming sediment is 10–20% sand<sup>2,27</sup>. Vegetative conditions that enhance sand deposition are important for resiliency because at least in the Mississippi River sand supply remains constant whereas humans are decreasing mud fluxes<sup>27</sup>. For a given flood, our results suggest that intermediate vegetation height and density are optimal for enhancing sand and mud deposition, whereas tall, dense vegetation forces sand into the channels, where it bypasses the deltaic marshes and causes shoreline accretion (Fig. 3). Shoreline accretion may increase delta size, although at the expense of vertical surface growth that combats relative sea-level rise.

Second consider that unlike tidal marshes, most sediment is delivered to freshwater deltaic marshes by infrequent events such as hurricanes and storms<sup>14</sup>, or river floods<sup>2,3</sup>. The integrated effect of vegetation on sedimentation in deltaic marshes then depends on event arrival relative to vegetation height and density. To illustrate this, notice that an NDVI time series for a marsh platform on the Wax Lake Delta, Louisiana, USA (Supplementary Fig. 4) shows that deltaic marsh vegetation has a pronounced cycle of growth and decay<sup>15</sup> (Fig. 4). The flood wave arrival varies relative to the vegetation wave: flooding from May to July 2011 occurs during relatively high NDVI values and may enhance mud deposition, whereas flooding from March to May 2010 occurs during lower NDVI and may enhance sand deposition (Fig. 4).

These ideas may help enhance sedimentation on drowning coastlines, such as Louisiana, USA. Although it is thought that the Mississippi Delta will inevitably drown owing to sea-level rise and lack of sediment supply<sup>4</sup>, recent efforts have shown that restoration scenarios are feasible<sup>2,3,28</sup>. These ecogeomorphic feedbacks may help improve restoration strategies and enhance deltaic resiliency.



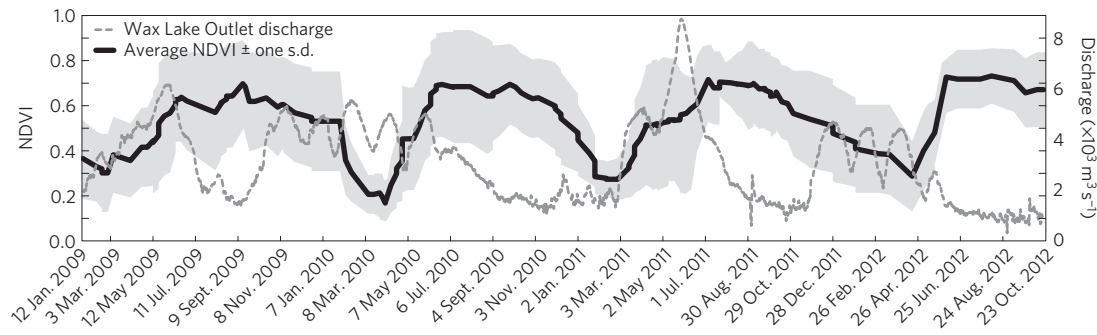


**Figure 4 | NDVI and flood hydrograph time series for Wax Lake Delta.** The thick black line shows spatially averaged NDVI and the grey envelope shows one standard deviation for a marsh platform of Wax Lake Delta, Louisiana, USA, from 12 January 2009 to 23 October 2012. The thin grey, dotted line is river discharge for Wax Lake Outlet at Calumet, Louisiana (discharge gauges USGS 07381590) over the same period. The NDVI time series is an average of all NDVI values within the marsh platform (Supplementary Fig. 4), and then smoothed with a 4-point moving average.

## Methods

**Model set-up.** To compute flow and sediment transport in deltaic environments we use Delft3D, which solves the three-dimensional equations for momentum and continuity for unsteady, incompressible, turbulent flow. The hydrodynamic and morphodynamic modules are fully coupled so that the flow field adjusts in real time as the bed topography changes. Our runs were computed using the depth-averaged version of the model. To generate our initial delta morphology, we simulate a river discharging into a basin, devoid of waves, tides and buoyancy forces. The delta is allowed to form until it reaches dynamic steady state, which we define as when the average topset slope stops changing. Simulations with vegetation are then restarted exactly from this bathymetric, and hydrodynamic state, but are not morphodynamic. The computations are performed on a grid of 500 by 750 cells, each of size  $10 \times 10$  m (Fig. 1). The basin had an initial slope of 0.0004, creating initial depths from 1 to 3.5 m comparable to the Wax Lake Delta, Louisiana. Initial depths are then adjusted from 0 to 5 cm using a white-noise model to simulate natural variations. A rectangular river channel of 250 m wide by 3 m deep and extending 500 m towards the basin is carved into a sandy shoreline along the southern boundary of the grid. Tests show that the shoreline width does not alter the numerical results. The lower, upper and left boundaries are open with a constant water surface elevation equal to zero (Fig. 1). Five metres of non-cohesive and cohesive sediment are initially available for erosion at the bottom of the domain.

For sediment transport we use the Van Rijn transport formulation for non-cohesive sediment and the Partheniades–Krone formulation for cohesive sediment (see Delft3D manual for full reference). The incoming sediment boundary conditions consist of equilibrium flux of non-cohesive sediment and a set concentration of cohesive sediment ( $0.5 \text{ kg m}^{-3}$ ) and suspended sediment eddy diffusivities are a function of the fluid eddy diffusivities and are calculated using horizontal large-eddy simulations and grain settling velocity. A time step of 6 s is adopted to satisfy all stability criteria. The horizontal eddy-viscosity coefficient is defined as the combination of the subgrid-scale horizontal eddy viscosity, computed from a horizontal large-eddy simulation, and the background horizontal viscosity here set equal to  $0.001 \text{ m}^2 \text{ s}^{-1}$ . Bed roughness is set to a spatially and temporally constant Chézy value of  $45 \text{ m}^{1/2} \text{ s}^{-1}$ .

We demarcate marsh platforms by tracing the zero-elevation contour around individual platforms. In each platform we calculate the incoming and outgoing water and sediment fluxes. The values will be accumulated over grid cells for which the centre point is located within the polygon.

To define the shoreline we applied an image-based method for mapping coasts proposed in ref. 29. The opening angle method uses visibility to define the shoreline. The shoreline is defined by the collection of points where open water is visible across an opening angle greater than a specified critical value.

**NDVI calculations and multivariate regression.** We calculate the NDVI index for 76 scenes from Landsat 4, 5 and 7 that make up the time series in Fig. 4 and the data set for the multiregression analysis. We use the US Geological Survey (USGS) level 2A product, which consists of atmospherically corrected reflectance data, to calculate NDVI with the red and near-infrared bands. We chose only images that present a cloud-free view of the marsh of interest (Supplementary Fig. 4). NDVI ranges from  $-1$  to  $1$ , where values above zero correspond to proportionally more vegetation greenness, and values below zero are open water.

For the multiregression, we selected NDVI scenes for those days that also had discharge, tide and water level measurement. We use observed daily averaged water level data on Wax Lake Delta from the USGS gauge 073815925 recorded

from 2009 to 2013. Daily averaged discharge data come from USGS gauge 07381590 located  $\sim 18$  km upstream. Tide data come from the Amerada Pass tide gauge and we use the tidal elevation that corresponds to the time of the Landsat scene (National Oceanic and Atmospheric Administration #11354 located  $\sim 4$  km east of Wax Lake Delta). We use NDVI as a proxy for vegetation abundance. The multiple regression equation, when compared with observed data, has an  $R^2 = 0.87$  (Supplementary Fig. 5). For the NDVI data in the multiregression, we average all of the pixels contained within the marsh platform at the head of the delta because it is closest to the stage gauge (Supplementary Fig. 4). As we are interested in the effect rough vegetated surface has on water level, we set all water pixels to 0 because the NDVI values from 0 to  $-1$  do not reflect changes in roughness.

Received 7 November 2013; accepted 21 July 2014;  
published online 24 August 2014

## References

- Syvitski, J. P. M. *et al.* Sinking deltas due to human activities. *Nature Geosci.* **2**, 681–686 (2009).
- Nittrouer, J. A. *et al.* Mitigating land loss in coastal Louisiana by controlled diversion of Mississippi River sand. *Nature Geosci.* **5**, 534–537 (2012).
- Falcini, F. *et al.* Linking the historic 2011 Mississippi River flood to coastal wetland sedimentation. *Nature Geosci.* **5**, 803–807 (2012).
- Blum, M. D. & Roberts, H. H. Drowning of the Mississippi Delta due to insufficient sediment supply and global sea-level rise. *Nature Geosci.* **2**, 488–491 (2009).
- Wilson, C. A. & Allison, M. A. An equilibrium profile model for retreating marsh shorelines in southeast Louisiana. *Estuar. Coast. Shelf Sci.* **80**, 483–494 (2008).
- Edmonds, D. A., Hoyal, C. J. D., Sheets, B. A. & Slingerland, R. L. Predicting delta avulsions: Implications for coastal wetland restoration. *Geology* **37**, 759–762 (2009).
- Jerolmack, D. J. Conceptual framework for assessing the response of delta channel networks to Holocene sea level rise. *Quat. Sci. Rev.* **28**, 1786–1800 (2009).
- Kirwan, M. L. & Megonigal, J. P. Tidal wetland stability in the face of human impacts and sea-level rise. *Nature* **504**, 53–60 (2013).
- Lesser, G., Roelvink, J., Van Kester, J. & Stelling, G. Development and validation of a three-dimensional morphological model. *Coastal Eng.* **51**, 883–915 (2004).
- Stumpf, R. P. The process of sedimentation on the surface of a salt marsh. *Estuar. Coast. Shelf Sci.* **17**, 495–508 (1983).
- Fagherazzi, S. *et al.* Numerical models of salt marsh evolution: Ecological, geomorphic, and climatic factors. *Rev. Geophys.* **50**, 2011RG000359 (2012).
- Rosen, T. & Xu, Y. J. Recent decadal growth of the Atchafalaya River Delta complex: Effects of variable riverine sediment input and vegetation succession. *Geomorphology* **194**, 108–120 (2013).
- Morris, J. T., Sundareshwar, P., Nietch, C. T., Kjerfve, B. & Cahoon, D. Responses of coastal wetlands to rising sea level. *Ecology* **83**, 2869–2877 (2002).
- Baumann, R. H., Day, J. W. & Miller, C. A. Mississippi deltaic wetland survival: Sedimentation versus coastal submergence. *Science* **224**, 1093–1095 (1984).
- Johnson, W., Sasser, C. & Gosselink, J. Succession of vegetation in an evolving river delta, Atchafalaya Bay, Louisiana. *J. Ecol.* **73**, 973–986 (1985).
- Edmonds, D. A. Restoration sedimentology. *Nature Geosci.* **5**, 758–759 (2012).

17. Baptist, M. *Modelling Floodplain Biogeomorphology* PhD thesis, Delft Univ. Technology (2005).
18. Nepf, H. M. Hydrodynamics of vegetated channels. *J. Hydraul. Res.* **50**, 262–279 (2012).
19. Crosato, A. & Saleh, M. S. Numerical study on the effects of floodplain vegetation on river planform style. *Earth Surf. Process. Landf.* **36**, 711–720 (2011).
20. Arboleda, A. M., Crosato, A. & Middelkoop, H. Reconstructing the early 19th-century Waal River by means of a 2D physics-based numerical model. *Hydrol. Process.* **24**, 3661–3675 (2010).
21. Baptist, M. *et al.* On inducing equations for vegetation resistance. *J. Hydraul. Res.* **45**, 435–450 (2007).
22. Mudd, S. M., D'Alpaos, A. & Morris, J. T. How does vegetation affect sedimentation on tidal marshes? Investigating particle capture and hydrodynamic controls on biologically mediated sedimentation. *J. Geophys. Res.* **115**, F03029 (2010).
23. Twilley, R. R. & Rivera-Monroy, V. Sediment and nutrient tradeoffs in restoring Mississippi River delta: Restoration vs eutrophication. *J. Contemp. Wat. Res. Educ.* **141**, 39–44 (2009).
24. Bennett, S. J., Pirim, T. & Barkdoll, B. D. Using simulated emergent vegetation to alter stream flow direction within a straight experimental channel. *Geomorphology* **44**, 115–126 (2002).
25. Temmerman, S. *et al.* Vegetation causes channel erosion in a tidal landscape. *Geology* **35**, 631–634 (2007).
26. Partheniades, E. Erosion and deposition of cohesive soils. *J. Hydraul. Div. ASCE* **91**, 105–139 (1965).
27. Nittrouer, J. A. & Viparelli, E. Sand as a stable and sustainable resource for nourishing the Mississippi River delta. *Nature Geosci.* **7**, 350–354 (2014).
28. Kim, W., Mohrig, D., Twilley, R., Paola, C. & Parker, G. Is it feasible to build new land in the Mississippi River Delta? *Eos Trans. AGU* **90**, 373–374 (2009).
29. Shaw, J. B., Wolinsky, M. A., Paola, C. & Voller, V. R. An image-based method for shoreline mapping on complex coasts. *Geophys. Res. Lett.* **35**, L12405 (2008).

### Acknowledgements

This work was financially supported by an NSF Frontiers in Earth Systems Dynamics grant (EAR-1135427), NSF grant OCE-1329542, and funds from the Alfred P. Sloan Foundation. We would like to thank S. Fagherazzi for insightful conversations about vegetation and sedimentation.

### Author contributions

All authors contributed equally in this research.

### Additional information

Supplementary information is available in the [online version of the paper](#). Reprints and permissions information is available online at [www.nature.com/reprints](http://www.nature.com/reprints). Correspondence and requests for materials should be addressed to W.N. or D.A.E.

### Competing financial interests

The authors declare no competing financial interests.